Optics Communications 412 (2018) 134–140

Contents lists available at ScienceDirect

Optics Communications

journal homepage: www.elsevier.com/locate/optcom

Optical emission spectroscopy of carbon laser plasma ion source

Oguzhan Balki [a], Md. Mahmudur Rahman [a], Hani E. Elsayed-Ali [a,b,*]

[a] Department of Electrical and Computer Engineering, Old Dominion University, Norfolk, VA 23529, USA
[b] Applied Research Center, 12050 Jefferson Avenue, Newport News, VA 23606, USA

A R T I C L E I N F O

Keywords:
Laser plasma
Ions source
Optical emission spectroscopy

A B S T R A C T

Carbon laser plasma generated by an Nd:YAG laser (wavelength 1064 nm, pulse width 7 ns, fluence 4–52 J cm^{-2}) is studied by optical emission spectroscopy and ion time-of-flight. Up to C^{4+} ions are detected with the ion flux strongly dependent on the laser fluence. The increase in ion charge with the laser fluence is accompanied by observation of multicharged ion lines in the optical spectra. The time-integrated electron temperature T_e is calculated from the Boltzmann plot using the C II lines at 392.0, 426.7, and 588.9 nm. T_e is found to increase from ~0.83 eV for a laser fluence of 22 J cm^{-2} to ~0.90 eV for 40 J cm^{-2}. The electron density n_e is obtained from the Stark broadened profiles of the C II line at 392 nm and is found to increase from $\sim 2.1 \times 10^{17}$ cm^{-3} for 4 J cm^{-2} to $\sim 3.5 \times 10^{17}$ cm^{-3} for 40 J cm^{-2}. Applying an external electric field parallel to the expanding plume shows no effect on the line emission intensities. Deconvolution of ion time-of-flight signal with a shifted Maxwell–Boltzmann distribution for each charge state results in an ion temperature T_i ~4.7 and ~6.0 eV for 20 and 36 J cm^{-2}, respectively.

1. Introduction

Laser multicharged ion (MCI) sources are attracting significant interest as they offer a pulsed, high flux source of ions from practically any solid [1]. Carbon ions are used in wide applications that include cancer therapy [2], deposition of diamond-like and carbide thin film [3,4], and ion implantation [5–8]. Carbon ion doping was shown to modify TiO_2 thin films, lowering the band-gap energy from 3.3 eV to 1.8 eV [4], thus, making it photocatalytically active to visible light. Carbon ion implantation on thin Ni film grown on a SiO_2/Si substrate was used for the synthesis of grapheme layers on top and under the Ni film [6]. Carbon ion implantation on high temperature growth of heteroepitaxial GeSn/Si and SiSn/Si structures was shown to suppress Sn segregation and precipitation, improve the thermal stability of SiSn supersaturated layers, and prevent dislocation in the formation of loops [7]. In these applications of carbon ions only the singly-charged C^{1+} ions were used. In some applications, the use of MCIs is attractive since their high potential energy is localized to the surface and they can be accelerated with reduced electrostatic field and bent and focused with reduced magnetic field.

Many techniques are used to probe plasma characteristics such as density n_e, electron temperature T_e, ion temperature T_i, and sheath potential. For pulsed plasma, *e.g.*, laser plasma, diagnostic techniques include optical emission spectroscopy (OES) [9], Thomson scattering [9], laser interferometry [10], and probing of ion emission from the laser plasma [11]. Laser-target interaction generates transient species such as excited atoms, molecules or ions, which emits radiation that includes the ultraviolet to near-infrared parts of the spectra. Line emission from laser plasma have been extensively used to diagnose n_e and T_e [12]. OES is widely used to probe n_e using Stark broadening of spectral lines, for n_e values ranging between 10^{14} and 10^{18} cm^{-3}, and to probe T_e using the ratio of integrated line intensities based on the Boltzmann's method for plasma in local thermal equilibrium (LTE) [13,14].

Several studies were conducted on carbon laser plasma. OES of carbon laser plasma in air generated by an Nd:YAG laser (pulse width $\tau = 5$ ns, frequency $F = 10$ Hz, wavelength $\lambda = 1064$ nm, maximum pulse energy $E = 130$ mJ/pulse, and for $\lambda = 532$ nm, maximum $E = 72$ mJ/pulse) [12]. The electron density n_e was calculated from the Stark broadening profile of the C I line at 247.85 nm. The electron temperature T_e was calculated from the neutral C I lines at 247.85, 394.22, 396.14, 588.95, and 591.25 nm. At a distance of 0.05 mm from the target surface, n_e was reported as 4.6×10^{17} cm^{-3} for 130 mJ at $\lambda = 1064$ nm, and 5.98×10^{17} cm^{-3} for 72 mJ at $\lambda = 532$ nm. The corresponding T_e values were 0.85 and 0.81 eV for the $\lambda = 1064$ and 532 nm laser radiance, respectively [15]. For ablation of graphite by an Nd:YAG laser ($\lambda = 1064$ nm, $F = 10$ Hz, intensity $I = 59$ GW cm^{-2}), n_e

* Corresponding author at: Department of Electrical and Computer Engineering, Old Dominion University, Norfolk, VA 23529, USA.
E-mail address: helsayed@odu.edu (H.E. Elsayed-Ali).

https://doi.org/10.1016/j.optcom.2017.11.087
Received 4 November 2017; Received in revised form 29 November 2017; Accepted 30 November 2017

and T_e were reported as 2.1×10^{17} cm^{-3} and 2.43 eV, respectively, at a distance 1 mm from the surface of the target decaying to 1×10^{17} cm^{-3} and 1.6 eV at 11 mm from the target surface for a laser radiance of 59 GW cm^{-2} [12]. Dual-laser ablation of carbon plasma (τ = 7 ns, 10 Hz, λ_1 = 1064 nm, λ_2 = 532 nm at fluence of 25 and 17 J cm^{-2}, respectively) showed up 5 fold intensification of C II emission lines for a delay of 500–1000 ns between the two laser pulses [16]. Changing the delay between the two laser pulses was shown to affect the ion kinetic energy. Ion time-of-flight (TOF) measurement and UV spectroscopy were conducted for the Al, Ti, Mo, and Au plasmas generated by irradiation with a Nd:YAG laser (τ = 3 ns, single-shot or up to 10 Hz, λ = 1064 nm, at a fluence up 18 J cm^{-2}) [17]. They probed the plasma plume by optical spectroscopy and deconvolution from TOF. For ablating with 18 J cm^{-2}, the reported ion temperatures for Al, Ti, Mo, Au, were 40, 41, 42, 44 eV, respectively. These values were obtained from deconvolution of the ion TOF signal based on a shifted Coulomb–Boltzmann distribution. The electron temperatures reported with optical spectroscopy were in the order of 1.0 eV. The difference in T_i and T_e was attributed to the different zones of the laser plasma where the ions and optical radiation were generated at [17].

We report on a combined OES and ion TOF study of carbon plasma generated by laser ablation using an Nd:YAG laser operating at λ = 1064 nm with τ = 7 ns. Time-integrated T_e and n_e are measured by OES, while ion TOF is used to obtain T_i. Carbon spectral lines up to C IV (C^{3+}) and carbon ions with charge states up to C^{4+} are observed for ablation by a laser fluence of ≥27 J cm^{-2}. The Stark-broadened profile of the singly-ionized C II line at 392.0 nm is used for the measurements of n_e, while the relative line intensities of the C II lines at 392.0, 426.7, and 588.9 nm are used to calculate T_e. Applying an external electric field parallel to the direction of plume propagation increases the carbon MCI extraction, however, no change in the carbon emission lines was observed.

2. Experimental

A schematic of the experimental setup is shown in Fig. 1. The vacuum chamber has a background pressure of ∼2×10^{-8} Torr. At such pressure, the loss of MCIs by charge transfer to the background gas over the transport line length is negligible [18]. A Q-switched Nd:YAG laser (Continuum Surelite SL I–10, τ = 7 ns, λ = 1064 nm, F = 4 – 52 J cm^{-2}) is used for plasma generation from a glassy carbon disk target of 5.8 mm thick, 99.99% purity, <50 nm surface roughness. The carbon target is electrically insulated from the chamber to allow applying a positive bias while the chamber is grounded. The laser pulse energy is controlled by a half-wave plate and a polarizing beam splitter. The laser pulse is incident on the target at an angle of 60° from the target normal and focused using a lens with a focal length of 200 mm to an elliptical spot on the surface of the target with an area of 0.1256 mm^2. The laser spot size was measured by scanning the laser spot with a knife edge parallel and perpendicular to the spot's major axis at target-equivalent plane in a direction 60° from the beam propagation direction. The reported laser fluences are adjusted for the losses in the BK7 glass window and the lens. A grounded nickel mesh 8 cm in diameter with an open area of 70% is placed 10 cm in front and parallel to the surface of the carbon disk. A voltage of 0–9 kV is applied to the carbon target using a high-voltage power supply (CPS Inc.,100-R, 30 kV, 1 mA) while keeping the chamber grounded. Ions with a range of kinetic energy-to-charge E/z ratios are selected by an electrostatic ion energy analyzer (EIA) with a radial cylindrical design at a deflection angle of 90°. The EIA has a range of E/z obtained by the relation $E/z = eU/[2\ln(R_2/R_1)]$, where E is the kinetic energy of the ion, e is the electron charge, U is the total potential across the plates, R_1 is the inner radius, and R_2 is the outer radius [19,20]. Ion entrance and exit slits can be placed in the EIA to reduce the spread in E/z selected. All results reported are without slits in order to increase ion transmission. The ions are detected by a Faraday cup (FC) made out of Al and placed 154 cm away from the carbon target. The ion transport line is a stainless-steel tube with 10 cm ID. The signal from secondary electron emission is suppressed by a suppressor ring electrode that is 5 cm in diameter placed 1 cm away from the FC entrance. The MCI TOF signal is detected with the FC biased at −80 V. The secondary electron emission signal from the FC due to positive ion collisions is found to be completely suppressed when biasing the suppressor electrode at −120 V. More details on the experimental setup were previously reported [21]. An oscilloscope (Tektronix DPO 3034, 50 Ω termination) records the carbon ion signals through a 0.66 μF coupling capacitor. For MCI TOF data collection, twenty consecutive laser pulses hitting the same target area are averaged in order to increase the signal-to-noise ratio. An optical spectrometer (Avantes, ULS3648) is used to record the spectral lines emitted from the carbon plasma. The carbon spectral emission is recorded through an optical fiber (Avantes, FC-UV-1000-1-ME) placed ∼15 cm away from the target at an angle of 60° from the target normal. The laser is operated at 10 Hz. The optical spectra are obtained by integrating for 20 s in a dark room. Background noise was recorded before any spectrum was acquired and subtracted from the optical spectra. The effect of applying an external electric field on the optical spectra is probed with another optical spectrometer (Avaspec-3648). This spectrometer covers the spectral range of 185–750 nm. In that case, the laser is operated at 1 Hz, while each spectrum is obtained by integrating the optical signal for 10 s. In this case, the optical feedthrough is replaced with a quartz viewport and a lens with focal length of 200 mm is used to image the plume onto the fiberoptic cable entrance.

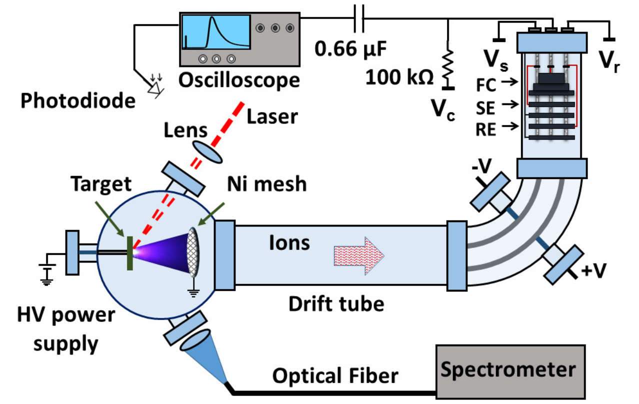

Fig. 1. A schematic of the experimental setup. The laser multicharged ion (MCI) chamber is connected to with a transport line with electrostatic ion analyzer (EIA), three-mesh retarding field analyzer (RFA), and time-of-flight (TOF) analyzer. V_r, V_s, and V_c are the voltage applied to the retarding electrode (RE) of the three-grid energy analyzer, suppressor electrode (SE), and Faraday cup (FC).

3. Results and discussions

3.1. Optical emission spectra

In this section, time-integrated optical emission spectra of the laser plasma are discussed. The effects of the laser fluence on the electron density n_e and electron temperature T_e are reported. We also report on the optical emission spectra when an external electric field is present across the laser plasma.

3.1.1. Lines intensities

The optical emission spectra obtained for different laser fluences are shown in Fig. 2. The carbon laser-plasma consists of ionization emission lines of C II, C III, and C IV transitions. A particular feature for the higher laser fluences is the increase in the intensities of all carbon lines and generation of higher ionization states. The line profile of the C^{1+} ion (C II at 392.0 nm) is used for the electron density n_e calculations. For